How to cite: *Angew. Chem. Int. Ed.* **2024**, *63*, e202319580
doi.org/10.1002/anie.202319580

Heterogeneous Catalysis | *Hot Paper*

Chloride and Hydride Transfer as Keys to Catalytic Upcycling of Polyethylene into Liquid Alkanes

*Wei Zhang, Hai Yao, Rachit Khare, Peiran Zhang, Boda Yang, Wenda Hu, Debmalya Ray, Jianzhi Hu, Donald M. Camaioni, Huamin Wang, Sungmin Kim, Mal-Soon Lee, Michele L. Sarazen, Jingguang G. Chen, and Johannes A. Lercher**

Abstract: Transforming polyolefin waste into liquid alkanes through tandem cracking-alkylation reactions catalyzed by Lewis-acid chlorides offers an efficient route for single-step plastic upcycling. Lewis acids in dichloromethane establish a polar environment that stabilizes carbenium ion intermediates and catalyzes hydride transfer, enabling breaking of polyethylene C–C bonds and forming C–C bonds in alkylation. Here, we show that efficient and selective deconstruction of low-density polyethylene (LDPE) to liquid alkanes is achieved with anhydrous aluminum chloride ($AlCl_3$) and gallium chloride ($GaCl_3$). Already at 60 °C, complete LDPE conversion was achieved, while maintaining the selectivity for gasoline-range liquid alkanes over 70 %. $AlCl_3$ showed an exceptional conversion rate of 5000 $g_{LDPE}\ mol_{cat}^{-1}\ h^{-1}$, surpassing other Lewis acid catalysts by two orders of magnitude. Through kinetic and mechanistic studies, we show that the rates of LDPE conversion do not correlate directly with the intrinsic strength of the Lewis acids or steric constraints that may limit the polymer to access the Lewis acid sites. Instead, the rates for the tandem processes of cracking and alkylation are primarily governed by the rates of initiation of carbenium ions and the subsequent intermolecular hydride transfer. Both jointly control the relative rates of cracking and alkylation, thereby determining the overall conversion and selectivity.

Introduction

Polyolefins, i.e., polyethylene and polypropylene, are the largest class of plastics produced globally. Their low cost, versatility, and durability have led to widespread use for single-use products such as plastic bags, packaging materials, and disposable masks.[1] However, this excessive consumption poses a long-term risk of environmental pollution, since polyolefins are highly resistant to degradation and end up in landfills or the environment.[2,3]

Ideally, such spent polyolefins could serve as hydrocarbon feedstocks, containing solely carbon and hydrogen.[4,5] It would require, however, a single stage process, which allows the integration in process paths for a diverse range of products including chemicals, intermediates, fuels, and lubricants, all suitable for existing end markets.[6–8]

Conventionally, the endothermic cleavage of C–C bonds in polyolefins presents a considerable challenge for upcycling.[9] Thermal and catalyst-aided cracking (pyrolysis, catalytic pyrolysis) demands substantial energy input and lacks precise control over product distribution, producing low-value hydrocarbon mixtures of gases, waxes, and chars.[10] To achieve complete conversion at low temperatures, kinetic coupling of the endothermic C–C cleavage with exothermic reactions such as hydrogenolysis,[11–18] hydrocracking,[19–21] cyclization[22–24] and metathesis is required.[25–29] This approach allows complete conversion at milder temperatures and may even reduce the overall free energy barrier.[30] While it has been used to overcome

---

[*] Dr. W. Zhang, B. Yang, Dr. W. Hu, Dr. D. Ray, Dr. J. Hu, Dr. D. M. Camaioni, Dr. H. Wang, Dr. S. Kim, Dr. M.-S. Lee, Prof. Dr. J. A. Lercher
Institute for Integrated Catalysis
Pacific Northwest National Laboratory (PNNL)
Richland, Washington 99354, USA
E-mail: johannes.lercher@ch.tum.de

Dr. W. Zhang, H. Yao, Dr. R. Khare, P. Zhang, Prof. Dr. J. A. Lercher
Department of Chemistry and Catalysis Research Center
Technical University of Munich (TUM)
Lichtenbergstrasse 4, 85747 Garching, Germany

Dr. J. Hu
The Gene and Linda Voiland School of Chemical Engineering and Bioengineering
Washington State University
Pullman, Washington 99164, USA

Asst. Prof. Dr. M. L. Sarazen
Department of Chemical and Biological Engineering
Princeton University, Princeton, New Jersey 08544, USA

Prof. J. G. Chen
Department of Chemical Engineering
Columbia University
New York,10027, USA

thermodynamic limitations with respect to sole cracking, challenging practical hurdles exist due to the limited chain mobility of molten polyolefins at lower temperatures, limiting access to catalytic sites, especially for multi-functional catalysts.[31]

Recently we developed a tandem cracking-alkylation strategy for transforming discarded polyolefins into gasoline-range iso-alkanes using a single-stage process catalyzed by acidic chloroaluminate-based ionic liquids at temperatures below 100 °C.[32] The process is initiated by the combination of Lewis acidic chloroaluminate ions and a small quantity of alkyl chloride additive. The latter generates in situ strong Lewis acidic species that abstract halogen anions and form carbenium ions. These carbenium ions undergo hydride transfer and, if this hydride transfer involves polymer chains, C–C bond cleavage in the polyolefin macromolecule. Subsequently, propagation occurs via the exothermic alkylation of isoparaffins (e.g., isopentane) with alkenes formed by cracking of polymer strands. Excellent hydride transfer leads to a relatively narrow product distribution and minimizes the production of red oil waste during the cascade cracking-alkylation of LDPE and iC_5. It should be noted that the strongly ionic environment induced by the polar environment enables cleavage of C–C bonds below 100 °C.

Motivated by these findings, we investigated whether only the ionic liquids or also a Lewis acidic catalyst consisting of abundant elements could be used to directly catalyze polyolefin conversion to alkylates at such temperatures. The underlying hypotheses was that Lewis acid-catalyzed hydride transfer (involved in both the endothermic and exothermic steps of cracking and alkylation cycles) is critical for catalytic activity and selectivity.

As a result, we present a study focused on the low-temperature activation of polyolefins in isopentane (the alkylating agent) using Lewis acidic catalysts derived from readily available elements, with the goal of identifying the specific properties of Lewis acid sites that are essential for this process. Notably, $AlCl_3$ exhibited the highest conversion rate of 5000 $g_{LDPE}\ mol_{cat}^{-1}\ h^{-1}$, surpassing all other tested Lewis acidic halides and triflates by more than an order of magnitude. This lack of reactivity is not directly correlated with the inherent strength of the Lewis acids or any potential steric hindrance that may interfere with interactions at the Lewis acid sites. Instead, it is shown to either stem from their inability to effectively initiate carbenium ions or, in cases where the carbenium ions are formed, from the inability of the Lewis sites to catalyze intermolecular hydride transfer. This transfer is indispensable for propagating the carbenium ions in the cracking and alkylation cycles.

Results and Discussion

Comparison of Lewis Acids

A wide range of Lewis acidic chlorides were investigated as catalysts for the deconstruction of low-density polyethylene (LDPE) via tandem cracking-alkylation. The catalyst pool included anhydrous metal chlorides (MCl_x) varying in valence states and electrophilicity (Figure S1a, Supporting Information). In a typical reaction, LDPE (200 mg) and isopentane (iC_5, 800 mg) were reacted in the presence of 1 mmol Lewis acid catalyst (together with 3 ml dichloromethane as solvent) at 70 °C for 30 min (Figure S1b). Most of the chlorides investigated showed only minor activity for LDPE transformation (including Cu^+, Mg^{2+}, Fe^{2+}, Co^{2+}, Zn^{2+}, Sn^{2+}, Cu^{2+}, In^{3+}, Bi^{3+}, Cr^{3+}, La^{3+}, Zr^{4+}, Hf^{4+}, Ti^{4+} and Mo^{5+}) and led to small amounts of wax (Figure S1c). In contrast, anhydrous $AlCl_3$ and $GaCl_3$ were remarkably active, achieving nearly quantitative LDPE conversion with high selectivity of gasoline-range liquid alkanes (over 70 %).Other products were gaseous isobutane (iC_4, ~18 wt %) and heavier alkanes (C_{13} to C_{40}, ~10 wt %). For comparison, the initial rates (calculated as grams of LDPE converted (at <20 % conversion) per hour and per mole of catalyst) are compiled in Figure 1a. Anhydrous $AlCl_3$ exhibited the highest rate, converting over 5000 $g_{LDPE}\ mol_{cat}^{-1}\ h^{-1}$ and outperforming $GaCl_3$ (400 $g_{LDPE}\ mol_{cat}^{-1}\ h^{-1}$). Most of the tested halides had initial conversion rates between of 40–100 $g_{LDPE}\ mol_{cat}^{-1}\ h^{-1}$, i.e., 2 orders of magnitude lower than that observed with $AlCl_3$. Temperature-dependent experiments (Figure 1, b–c) demonstrated the high activity of anhydrous $AlCl_3$ and $GaCl_3$ in LDPE conversion even under ambient conditions. $AlCl_3$, for example, converted approximately 60 % LDPE in 120 minutes at 30 °C; increasing the temperature to 70 °C led to a full conversion within 10 mins. It should be noted that the differences in maximum conversion at different temperatures are not related to deactivation of the catalysts but caused by thermodynamic limitations.

Properties Governing the LDPE Conversion with Lewis Acid Catalysts

The considerable variance in the properties of chlorides raises a crucial question about the necessary chemical and physical characteristics of MCl_x compounds, particularly those that enable them to catalyze the combined reactions of isomerization, cracking, and alkylation in a single-step process.

To address this question, we investigated the LDPE conversion catalyzed by group 13 halides in more detail (Figure S2). Although boron (B) and indium (In) also belong to Group 13 like Al and Ga, both showed very low rates of conversion. As the Lewis acid strength decreases in the order $BCl_3 > AlCl_3 > GaCl_3 > InCl_3$ we reasoned that Lewis acid strength is not determining the overall conversion rate. In the next step, the investigations were expanded to include a wider range of commonly used Lewis acids (Figure 2, a–c). The selected Lewis acids share either the same metal center, but are coordinated to anions of different electronegativity (halides vs. triflates) or have the same anion but a different metal center. In order to quantify the Lewis acid strength,[33] we used three scales of Lewis acidity, i.e., the Gutmann acceptor number (AN),[34]

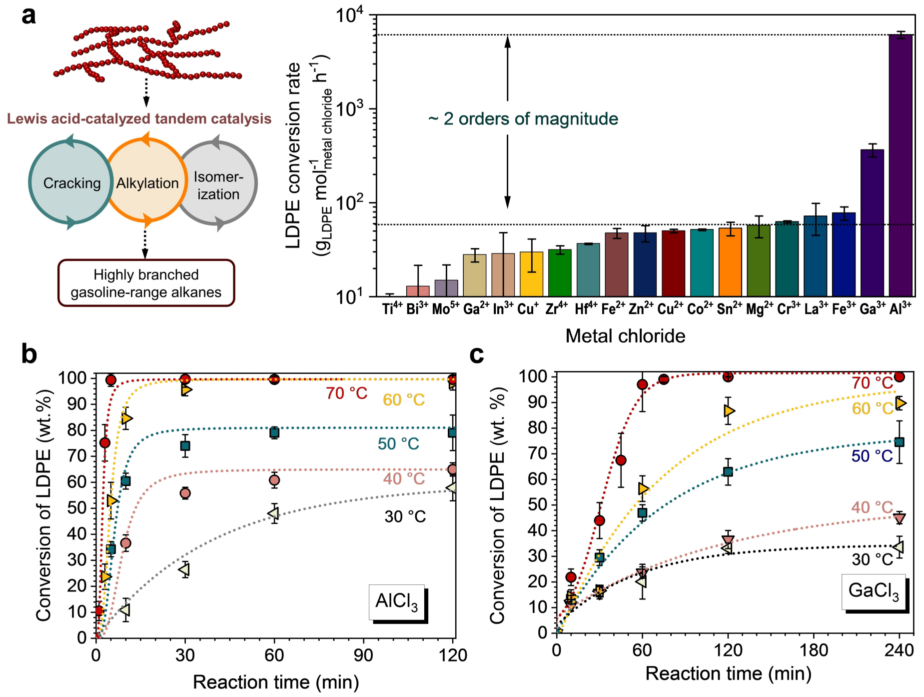

Figure 1. (**a**) Comparison of LDPE conversion rate over various metal chlorides. Reaction conditions: LDPE, 200 mg; iC_5, 800 mg; MCl_x, 0.1–1 mmol; DCM solvent, 3 ml; 60 °C, 30 min. (**b–c**) Time-resolved conversion profile of LDPE catalyzed by $AlCl_3$ (b) and $GaCl_3$ (c) at different temperatures, respectively. All data were repeated at least five times and are shown as mean data points. Catalyst loading: 0.5 mmol $AlCl_3$ or $GaCl_3$.

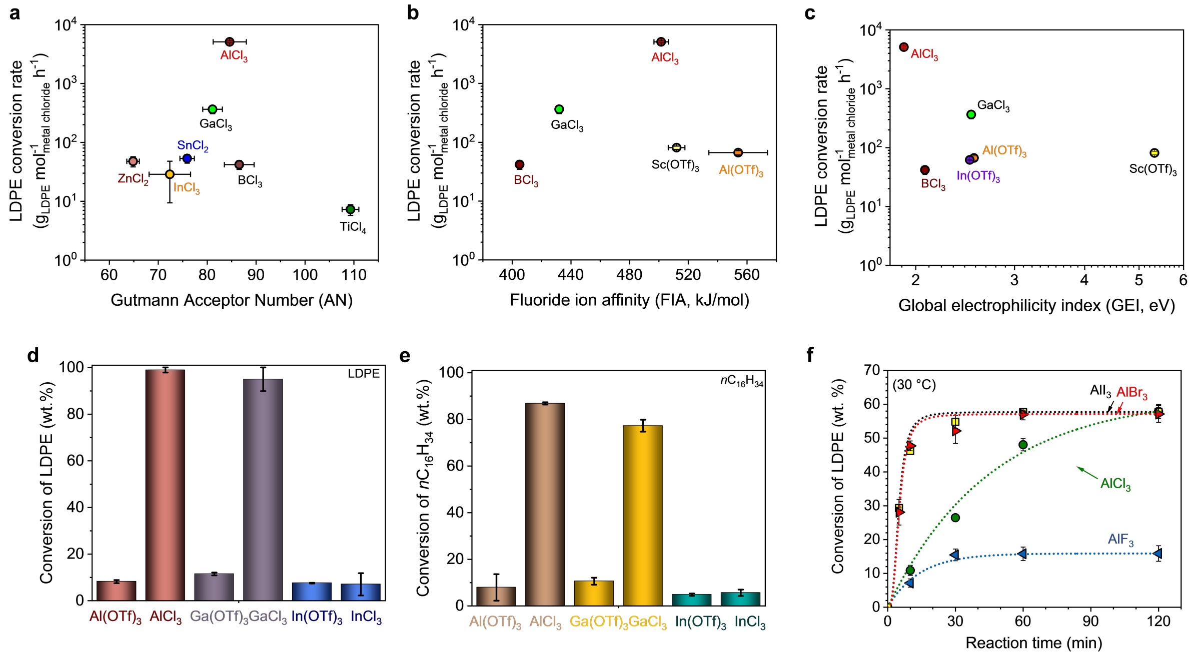

Figure 2. Factors governing the LDPE and n-hexadecane conversion on various Lewis acid catalysts. (**a–c**) Effect of Lewis acidity: The initial LDPE conversion rates plotted against Lewis acidity using three widely recognized Lewis acidity scaling methods: (a) Gutmann acceptor number (AN), (b) Fluoride ion affinity (FIA)and (c) Global electrophilicity index (GEI). Effect of steric hindrance: (**d--e**) Conversion of LDPE and n-hexadecane(n-$C_{16}H_{34}$) over group 13 chlorides and triflates, respectively; (**f**) Catalytic performance of various aluminum halides, including F, Cl, Br and I. Reaction conditions: 200 mg LDPE/n-$C_{16}H_{34}$, 800 mg iC_5, 1 mmol catalyst, 3 ml DCM, 30 °C.

the fluoride ion affinity (FIA),[35] and the global electrophilicity index (GEI).[36] Figure 2, a–c show, however, that the initial rates were unaffected by the Lewis acid strength, with only $AlCl_3$ and $GaCl_3$ showing high rates.

Further, while triflates have higher Lewis acid strength, they showed lower activity in both LDPE and n-$C_{16}H_{34}$ conversions, compared to the corresponding chlorides ($AlCl_3 > Al(OTf)_3$ and $GaCl_3 > Ga(OTf)_3$, Figure 2, d–e). Interestingly, larger halides such as Br and I exhibited higher reaction rates for the conversion of t n-$C_{16}H_{34}$ than the smaller halogen anions ($AlI_3 \approx AlBr_3 > AlCl_3 \gg AlF_3$) (Figure 2f). This sequence of reactivity suggests that the softer and more polarizable character of the large anions in the halogenide leads to more favorable transition states in the hydride transfer reactions.

Kinetic Model of LDPE Deconstruction on Aluminum Halides

Figure S3 a–b shows the initial LDPE conversion rates (r) as a function of concentrations of LDPE and iC_5 over the anhydrous $AlCl_3$ catalyst at room temperature, respectively. The rates normalized to the Al loading increased with the initial concentration of LDPE and iC_5. The slope refers to the apparent reaction orders with respect to LDPE and iC_5. The initial conversion rates (r) can be expressed, therefore, in a power rate law as:

$$r = k_L \bullet [C_nH_{2n+2}]^m \bullet [iC_5H_{12}]^n \qquad (1)$$

where the exponents m and n are the partial orders of LDPE and isopentane, respectively, with k_L being the lumped apparent rate constant. The measured reaction orders in LDPE and iC_5 are 0.84 ± 0.07 and $\sim 0.12 \pm 0.03$, respectively. The observed fractional order indicates that the adduct species are partly associated with activated reacting molecules and/or quasi-equilibrated intermediates. It should be noted that the dependence of the reaction rate on the conversion of n-$C_{16}H_{34}$ (0.8) was almost identical to that of LDPE, indicating that the substantial steric hindrance of LDPE/ n-$C_{16}H_{34}$ reduced the interaction of active sites, in contrast to iC_5.

The relationship between the apparent rate constant and the reaction temperature can be expressed as:

$$\ln\left(\frac{k}{T}\right) = -\frac{\Delta H^{o\ddagger}}{R} \cdot \frac{1}{T} + \ln\left(\frac{k_B}{h}\right) + \frac{\Delta S^{o\ddagger}}{R} \qquad (2)$$

Where ΔH^{o+} and ΔS^{o+} are enthalpy and entropy, respectively, k_B is Boltzmann constant, h is Planck constant, R is gas constant and T is temperature. ΔH^{o+} and ΔS^{o+} can be determined by plotting $\ln\left(\frac{k}{T}\right)$ against 1/T. An Eyring analysis over a temperature range of 30–70 °C gave the activation parameters including enthalpies ($\Delta H^{o\ddagger}$) and entropies of activation ($\Delta S^{o\ddagger}$), and their values are summarized in Table S1.

Despite the conversion rates of LDPE varying with different Al halides, plotting the logarithmic correlation between the initial conversion rates of LDPE and n-$C_{16}H_{34}$ as a model reactant against the inverse temperature (Figure S4) showed a consistent activation energy range of 40–44 kJ/mol. These values are similar to the activation energies for the hydride transfer reaction between two isobutane molecules (55 kJ/mol),[37] but significantly lower than the reported activation energy barrier for polyethylene depolymerization, which spans a range of 160–310 kJ/mol.[38,39] This observation suggests that the underlying mechanism and rate-limiting steps are consistent across the examined aluminum halides. The congruence of the activation energy with that of hydride transfer processes led us to hypothesize that the hydride transfer represented the pivotal step in this reaction sequence. Notably, the aluminum halides demonstrated significant catalytic efficacy even at lower temperatures, effectively reducing the activation energy barrier and thereby enhancing the rate of catalytic deconstruction of LDPE/ n-$C_{16}H_{34}$.

We should note that anhydrous $AlCl_3$ rapidly dissolves in our catalyst system, whereas $GaCl_3$ undergoes a noticeable physical transformation, transitioning from a white crystalline powder to larger, spherically aggregated forms. The apparent activation energies for the LDPE and n-$C_{16}H_{34}$ reactions involving $GaCl_3$ were found to be 16 and 23 kJ/mol, respectively (Table S1). These low values are speculated to be influenced by diffusion, which is governed by much lower activation energies.

In addition, we assessed the catalytic stability of $AlCl_3$ by conducting tests where LDPE was refilled every 30 minutes, allowing for approximately full conversion. We observed that the $AlCl_3$ catalyst retained its activity and could be reused without regeneration for at least three cycles, consistently achieving full LDPE conversion in each cycle and without influencing the initial conversion rates (Figure S5).

Ability to form Carbenium Ions

We have demonstrated that chloroaluminate ionic liquids are effective in deconstructing polyolefins into gasoline-range alkanes via tandem cracking-alkylation.[32] However, this requires the introduction of small amounts of *tert*-butyl chloride (TBC) as an additive. Intriguingly, anhydrous $AlCl_3$ showed greater activity than the corresponding ionic liquids and did not require the addition of TBC as the carbenium ion initiator (Figure 3a).

The difference between these systems lies in the concentration of $AlCl_3$. In the case of chloroaluminate ionic liquids catalyzed system, the dominating $Al_2Cl_7^-$ reacts with TBC via chloride abstraction, resulting in the formation of the $AlCl_3$ adducts ($AlCl_3 \cdots Cl \cdots iC_4$). These adducts rapidly convert into reactive ion-pair species, i.e., *tert*-butyl carbenium ions and $AlCl_4^-$. The initial carbenium ions subsequently activate the C–H bonds of reacting molecules (LDPE and iC_5) through successive hydride transfers, promoting the propagation of carbenium ions.

Computational simulations (Figure 3, b–c) showed that $Al_2Cl_7^-$ is more likely to react with TBC ($\Delta G^o = 23$ kJ/mol), exhibiting an equilibrium constant of 10^{-3}, which is significantly higher than its reaction with the DCM solvent which shows an equilibrium constant of 10^{-5} ($\Delta G^o = 31$ kJ/mol). The high concentration of $AlCl_3$ (give a comparison

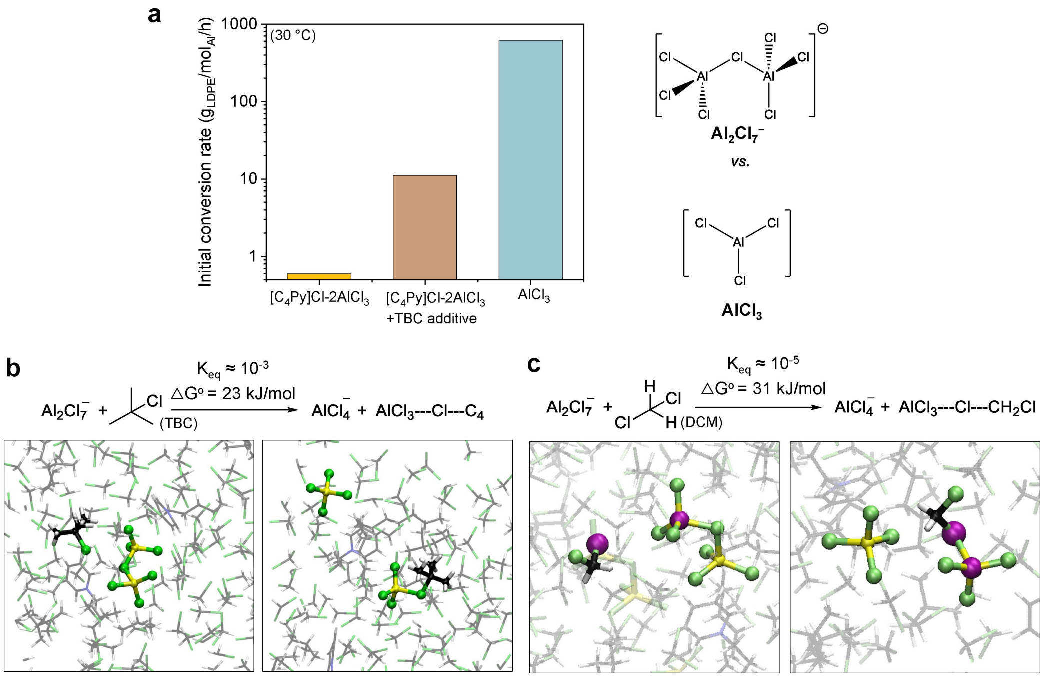

Figure 3. (**a**) Comparison of initial reaction rate over anhydrous $AlCl_3$, and $[C_4Py]Cl\text{-}2AlCl_3$ ionic liquid (with/without TBC additive). Reaction conditions: 200 mg LDPE, 800 mg iC_5, 3 ml DCM. Catalyst: 0.5 mmol $AlCl_3$ *vs.* 2 mmol $[C_4Py]Cl\text{-}2AlCl_3$ (with TBC 0.05 mmol).(**b–c**) Ab initio molecular dynamics simulations (Blue Moon ensemble method) of $Al_2Cl_7^-$reacting with tert-butyl chloride (TBC) and dichloromethane (DCM) to form $AlCl_3$ complexes, respectively. Images illustrate atomic configurations of the initial and final states.

to the calculated concentration in the ionic liquid) (over)compensates the low rate constant of DCM compared to TBC and induces higher rates than found with the ionic liquids. Thus, we hypothesize that anhydrous $AlCl_3$ directly interacts with DCM to form an active adduct, which subsequently undergoes hydride transfer with iC_5 and the polymer. It is known that DCM reacts with Lewis acids, i.e., is polarized by $AlCl_3$/$GaCl_3$, forming an electron donor-acceptor complex ($MCl_3 \leftarrow ClCH_2Cl$).[40,41] This complex can subsequently transform into a chloromethyl-carbenium ion and MCl_4^- pair,[42] represented as $[CH_2Cl]^+$ $[MCl_4]^-$ that initiates the reaction following carbenium ion chemistry.[43]

To corroborate this hypothesis, in situ ^{27}Al MAS NMR spectra were used to identify the aluminum species present in a dichloromethane (DCM) (Figure 4). The signals observed at 0 ppm were ascribed to solid $AlCl_3$ powder. Upon the addition of DCM, two distinct peaks were observed at 92 ppm and 99 ppm, corresponding to Al_2Cl_6 species and the $AlCl_3$-DCM complex, respectively.[44,45] An excessive amount of solid $AlCl_3$ in DCM resulted in prominent peaks at 0 ppm and 99 ppm, suggesting that Al_2Cl_6 coordinated with DCM to form an increased amount of the $AlCl_3$-DCM complex ($AlCl_3 \leftarrow ClCH_2Cl$), as illustrated by the equilibrium: Al_2Cl_6 (92 ppm) + $2CH_2Cl_2 \rightleftharpoons 2AlCl_3\text{-}CH_2Cl_2$ (99 ppm). This observation is consistent with the findings of Wu et al. regarding the associations in $AlCl_3$–arene solutions.[44] Introducing iC_5 to the mixture affects the anhydrous $AlCl_3$ solubility, as evidenced by the signal at 0 ppm. Notably, it also results in an increase in the resonance intensity at 99 ppm and a concurrent decrease in the Al_2Cl_6 signal at 92 ppm. The effect stems from a reaction with iC_5 (Figure S6), resulting in the formation of monomeric $AlCl_3$ adducts, detectable at approximately 99 ppm.

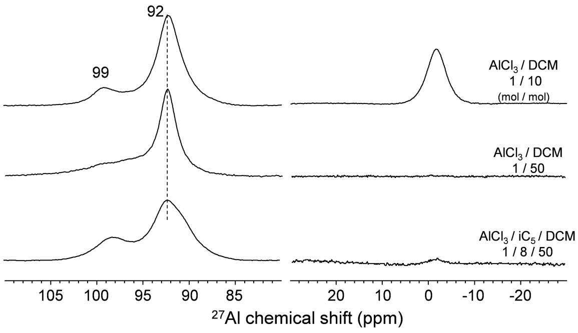

Figure 4. In situ ^{27}Al MAS NMR on anhydrous $AlCl_3$ in DCM solutions at room temperature.

Despite their strongly varying electron affinity, electrophilicity, and electronegativity, most of the tested Lewis acids remain inactive for the tandem cracking-alkylation of LDPE-iC_5. This is tentatively attributed to their inability to form a complex with DCM or, once formed, the resulting complex remains too stable to dissociate into ion pairs.

To test this hypothesis, we used TBC and iC_5 as model substrates with several Lewis acids. TBC allows for a significantly more facile formation of *tert*-carbenium ions (iC_4^+) via chloride abstraction, compared to DCM. The overall reaction involves a series of cascade reactions including dechlorination, isomerization, deprotonation, hydride transfer, and alkylation. For instance, iC_4^+ carbenium ion is initially formed from TBC via chloride abstraction, undergoes intermolecular hydride transfer with iC_5 to generate iC_5^+ and isobutane (iC_4); in parallel, the carbenium ion intermediates may also form the corresponding alkenes (e.g., $C_4^=$ and $C_5^=$) via deprotonation. Consequently, "self-alkylation" can occur via the addition of alkyl carbenium ions to alkenes ($iC_{\geq 4}^+ + C_{\geq 4}^=$), forming branched $C_{\geq 8}^+$ carbocations and the corresponding alkanes.

Figure 5a compares the catalytic efficacy of various metal salts for chloride abstraction of TBC. As expected, although most of the tested Lewis acidic compounds were inactive for both LDPE and n-$C_{16}H_{34}$ conversion, but demonstrate good catalytic activity for TBC transformation. For instance, $TiCl_4$, $MoCl_5$, and $FeCl_3$ led to moderate to high conversions, with approximately 40 %, 60 %, and 80 %, respectively; $ZrCl_4$, $HfCl_4$, $GaCl_2$, $Ga(OTf)_3$ and $In(OTf)_3$ achieved full TBC conversion, comparable to anhydrous $AlCl_3$ and $GaCl_3$. The major products comprised of a mixture of iso-alkanes ranging from C_4 to C_{12} (Figure 5b), which agrees with the hypothesis that consecutive alkylation-cracking occurs in the presence of a carbenium initiator. The selectivity of $C_{\geq 8}$ alkanes ranged from 35 % to 51 % for $FeCl_3$, $TiCl_4$, $MoCl_5$, and $In(OTf)_3$, whereas $ZrCl_4$, $HfCl_4$, $GaCl_3$ and $Ga(OTf)_3$ led to selectivity below 25 %. The high selectivity towards $C \geq 8$ with the former catalysts indicates that their cracking rate constants are relatively lower than the rate of intermolecular hydride transfer.

Based on these experiments, we conclude that the initial carbenium ions are prerequisite to initiate the overall reaction. Moreover, the consecutive hydride transfer between carbenium ions and reacting molecules enables the propagation of carbenium ions and determines the relative rates of cracking and alkylation. These rates, in turn, govern the selectivity and overall LDPE conversion (Figure S1).

Ability to Catalyze Hydride Transfer

To elucidate the mechanistic intricacies and kinetic parameters with which the Lewis acidic catalysts facilitate hydride transfer between carbenium ions and polymer chains, we substituted the alkylation agent, iC_5, with TBC. Concurrently, n-$C_{16}H_{34}$ was employed as a model reactant, serving as a simplified analog for polyethylene. With the addition of *tert*-butyl chloride, *tert*-butyl carbenium ions are easily formed. This bypasses the need for the initial formation of the chloromethyl-carbenium ion from DCM.

The substitution ensures the formation of initial *tert*-butyl carbenium ions (C_4^+) from TBC. Once intermolecular hydride transfer occurs between n-$C_{16}H_{34}$ and C_4^+ species, the resulting C_{16}^+ will either undergo isomerization or convert to its corresponding alkyl chlorides. Consequently, the rate of intermolecular hydride transfer for the catalysts, defined as mol of n-$C_{16}H_{34}$ converted per mol of catalyst per minute under identical conditions, are shown in Figure 5c. Note that most of the catalysts, such as $FeCl_3$ $MoCl_5$, $TiCl_4$ and $Ga(OTf)_3$ show low rates of intermolecular hydride transfer. Therefore, while these metal salts effectively generate carbenium ions through chloride abstraction from *tert*-butyl chloride (*c.f.*, Figure 5a), their slow catalysis of hydride transfer does not lead to appreciable formation of C_{16}^+. Consequently, this results in an effective inhibition of the conversion of n-$C_{16}H_{34}$. In contrast, $ZrCl_4$ and $HfCl_4$ exhibit a notably high rate of intermolecular hydride transfer, which is only slightly lower than that observed with $GaCl_3$. Thus, we conclude that intermolecular hydride transfer is pivotal in maintaining carbenium pathways in the cracking and alkylation cycles.

Conclusions

Only $AlCl_3$ and $GaCl_3$ catalyze selective deconstruction of LDPE to liquid alkanes close to ambient temperature. Both $AlCl_3$ and $GaCl_3$ form an electron donor-acceptor complex with DCM (e.g., $AlCl_3 \leftarrow ClCH_2Cl$), identifying it as a critical component in the catalytic system (Scheme 1). These complexes may evolve into a chloromethyl-carbe-

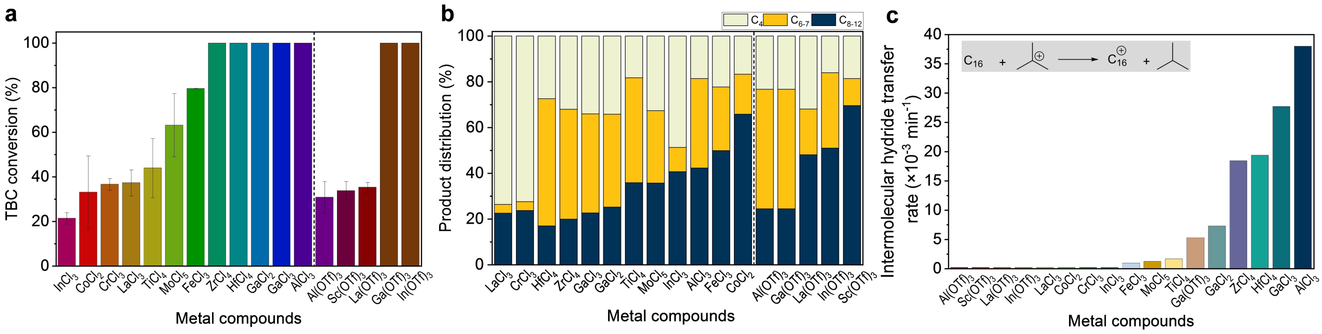

Figure 5. (**a**–**b**) Comparison of *tert*-butyl chloride conversion with various chlorides and triflates and the corresponding product distribution over selected metal compounds with 100 % *tert*-butyl chloride conversion. Reaction conditions: 200 mg *tert*-butyl chloride, 800 mg iC_5, 1 mmol Catalyst, 3 ml DCM, 70 °C, 30 min. (**c**) Comparison of n-$C_{16}H_{34}$ conversion with *tert*-butyl chloride over various metal chlorides. Reaction conditions: 1 mmol n-$C_{16}H_{34}$, *tert*-butyl chloride/ n-$C_{16}H_{34}$ = 1,1 mmol MCl_x, 3 ml DCM, 70 °C, 30 min (Note: a-c, reaction temperature 30 °C with $AlCl_3$).

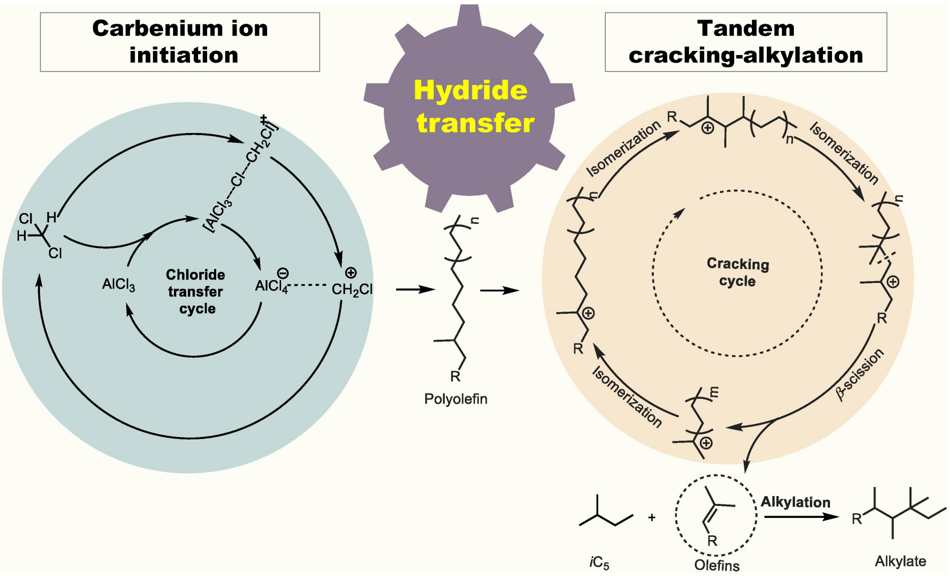

Scheme 1. Simplified catalytic cycle for the anhydrous $AlCl_3$ catalyzed tandem cracking and alkylation of polyolefin and isopentane in the presence of DCM. This includes the proposed reaction pathways for initiation of carbenium ions from DCM, as well as the progression of the cracking and alkylation cycles governed by hydride transfer.

nium ion and MCl_4^- pair ($[CH_2Cl]^+[AlCl_4]^-$), initiating the carbenium ion chemistry. Intermolecular hydride transfer is then critical for propagating the carbenium ions in the cracking and alkylation cycles along with concurrent isomerization. This conclusion was further corroborated through control experiments using n-$C_{16}H_{34}$ and TBC as model reactants. All tested materials were able to form carbenium ions by chloride abstraction to some degree.

With $Ga(OTf)_3$, $MoCl_5$, $TiCl_4$, $FeCl_3$, the introduction of TBC leads to the formation of *tert*-butyl carbenium ions, bypassing the need for the generation of the chloromethylcarbenium ion from DCM. But despite the ability to form carbenium ions by chloride abstraction from TBC, these materials catalyze hydride transfer only with very low rates. Consequently, they are practically unable to produce carbenium ions (with n-$C_{16}H_{34}$and LDPE) and are, hence, catalytically inactive.

Thus, we conclude that while both the formation of carbenium ions by chloride abstraction and the hydride transfer are necessary, the former is the easier criterion to be fulfilled. It is remarkable that Al^{3+} appears to be by far the best suited to catalyze this elementary step. It is also notable that the softer and more polarizable nature of the halogenide leads to a higher rate of this hydride transfer.

Thecurrent work shows that the key catalytic transformations coupled within one stage follows the same mechanism for polyolefins in their native pure forms and for model substrates based on linear paraffins (e.g., n-hexadecane). The identical nature of the active sites with $AlCl_3$ and the ionic liquids discussed previously convinces us that thisproof-of-concept demonstrations are applicable also to other types of polymers and practical polymers composites.We have shown previously that the catalytic chemistry is identical for different types of polymers with such catalysts.[32] The main difference between the different polymers lies in the accessibility to form carbenium ions, with crystalline HDPE reacting more slowly than LDPE, but leading to identical products; PP reacts faster and crosslinking leads to lower rates. The insight reported provides a path for developing further robust and economically viable catalysts for highly efficient low-temperature upcycling of polyolefin waste.

Supporting Information

The authors have cited additional references within the Supporting Information (Ref. [46–50]).

Acknowledgements

We thank G. L. Haller (Yale University) for his discussion of the manuscript and helpful suggestions. J.A.L., J.G.C., M. L. S., W.Z., H.W., S.K., J.H., W.H., J.M., B.Y., D.M.C. and M.-S.L. thank the U.S. Department of Energy (DOE), Office of Science, Office of Basic Energy Sciences (BES), Division of Chemical Sciences, Geosciences and Biosciences (Towards a polyolefin-based refinery: understanding and controlling the critical reaction steps, FWP 78459) for funding support. J.H also thankthe U.S. Department of Energy (DOE), Office of Science, Office of Basic Energy Sciences (BES), Division of Chemical Sciences, Geosciences and Biosciences (Multifunctional Catalysis to Synthesize and Utilize Energy Carrier, FWP 47319) for funding support of in situ NMR work. Open Access funding enabled and organized by Projekt DEAL.

Conflict of Interest

The authors declare no conflict of interest.

Data Availability Statement

The data that support the findings of this study are available from the corresponding author upon reasonable request.

Keywords: polyethylene upcycling · liquid alkanes · Lewis acid · carbenium ion · hydride transfer

---

[1] J. M. Garcia, M. L. Robertson, *Science* **2017**, *358*, 870–872.
[2] R. Geyer, in *Plastic Waste and Recycling* (Ed.: T. M. Letcher), Academic Press, **2020**, pp. 13–32.
[3] R. Geyer, J. R. Jambeck, K. L. Law, *Sci. Adv.* **2017**, *3*, e1700782.
[4] J. Sun, Y.-H. Lee, R. D. Yappert, A. M. LaPointe, G. W. Coates, B. Peters, M. M. Abu-Omar, S. L. Scott, *Chem* **2023**, *9*, 2318–2336.
[5] J.-P. Lange, *ACS Sustainable Chem. Eng.* **2021**, *9*, 15722–15738.
[6] C. W. S. Yeung, J. Y. Q. Teo, X. J. Loh, J. Y. C. Lim, *ACS Mater. Lett.* **2021**, *3*, 1660–1676.
[7] D. P. Serrano, J. Aguado, J. M. Escola, *ACS Catal.* **2012**, *2*, 1924–1941.
[8] T. Tan, W. Wang, K. Zhang, Z. Zhan, W. Deng, Q. Zhang, Y. Wang, *ChemSusChem* **2022**, *15*, e202200522.
[9] I. Vollmer, M. J. F. Jenks, M. C. P. Roelands, R. J. White, T. van Harmelen, P. de Wild, G. P. van der Laan, F. Meirer, J. T. F. Keurentjes, B. M. Weckhuysen, *Angew. Chem. Int. Ed.* **2020**, *59*, 15402–15423.
[10] A. J. Martín, C. Mondelli, S. D. Jaydev, J. Pérez-Ramírez, *Chem* **2021**, *7*, 1487–1533.
[11] J. E. Rorrer, G. T. Beckham, Y. Román-Leshkov, *JACS Au* **2020**, *1*, 8–12.
[12] C. Wang, T. Xie, P. A. Kots, B. C. Vance, K. Yu, P. Kumar, J. Fu, S. Liu, G. Tsilomelekis, E. A. Stach, W. Zheng, D. G. Vlachos, *JACS Au* **2021**, *1*, 1422–1434.
[13] C. Jia, S. Xie, W. Zhang, N. N. Intan, J. Sampath, J. Pfaendtner, H. Lin, *Chem Catal.* **2021**, *1*, 437–455.
[14] L. Chen, L. C. Meyer, L. Kovarik, D. Meira, X. I. Pereira-Hernandez, H. Shi, K. Khivantsev, O. Y. Gutiérrez, J. Szanyi, *ACS Catal.* **2022**, *12*, 4618–4627.
[15] P. A. Kots, T. Xie, B. C. Vance, C. M. Quinn, M. D. de Mello, J. A. Boscoboinik, C. Wang, P. Kumar, E. A. Stach, N. S. Marinkovic, L. Ma, S. N. Ehrlich, D. G. Vlachos, *Nat. Commun.* **2022**, *13*, 5186.
[16] C. Wang, K. Yu, B. Sheludko, T. Xie, P. A. Kots, B. C. Vance, P. Kumar, E. A. Stach, W. Zheng, D. G. Vlachos, *Appl. Catal. B* **2022**, *319*, 121899.
[17] G. Zichittella, A. M. Ebrahim, J. Zhu, A. E. Brenner, G. Drake, G. T. Beckham, S. R. Bare, J. E. Rorrer, Y. Román-Leshkov, *JACS Au* **2022**, *2*, 2259–2268.
[18] G. Celik, R. M. Kennedy, R. A. Hackler, M. Ferrandon, A. Tennakoon, S. Patnaik, A. M. LaPointe, S. C. Ammal, A. Heyden, F. A. Perras, M. Pruski, S. L. Scott, K. R. Poeppelmeier, A. D. Sadow, M. Delferro, *ACS Cent. Sci.* **2019**, *5*, 1795–1803.
[19] S. Liu, P. A. Kots, B. C. Vance, A. Danielson, D. G. Vlachos, *Sci. Adv.* **2021**, *7*, eabf8283.
[20] J. E. Rorrer, A. M. Ebrahim, Y. Questell-Santiago, J. Zhu, C. Troyano-Valls, A. S. Asundi, A. E. Brenner, S. R. Bare, C. J. Tassone, G. T. Beckham, Y. Román-Leshkov, *ACS Catal.* **2022**, *12*, 13969–13979.
[21] Q. Zhou, D. Wang, Q. Wang, K. He, K. H. Lim, X. Yang, W.-J. Wang, B.-G. Li, P. Liu, *Angew. Chem. Int. Ed.* **2023**, *n/a*, e202305644.
[22] F. Zhang, M. Zeng, R. D. Yappert, J. Sun, Y.-H. Lee, A. M. LaPointe, B. Peters, M. M. Abu-Omar, S. L. Scott, *Science* **2020**, *370*, 437–441.
[23] J. Du, L. Zeng, T. Yan, C. Wang, M. Wang, L. Luo, W. Wu, Z. Peng, H. Li, J. Zeng, *Nat. Nanotechnol.* **2023**, *18*, 772–779.
[24] J. H. Miller, A. K. Starace, D. A. Ruddy, *ChemSusChem* **2022**, *n/a*, e202200535.
[25] X. Jia, C. Qin, T. Friedberger, Z. Guan, Z. Huang, *Sci. Adv.* **2016**, *2*, e1501591.
[26] N. M. Wang, G. Strong, V. DaSilva, L. Gao, R. Huacuja, I. A. Konstantinov, M. S. Rosen, A. J. Nett, S. Ewart, R. Geyer, S. L. Scott, D. Guironnet, *J. Am. Chem. Soc.* **2022**, *144*, 18526–18531.
[27] R. J. Conk, S. Hanna, J. X. Shi, J. Yang, N. R. Ciccia, L. Qi, B. J. Bloomer, S. Heuvel, T. Wills, J. Su, A. T. Bell, J. F. Hartwig, *Science* **2022**, *377*, 1561–1566.
[28] A. Arroyave, S. Cui, J. C. Lopez, A. L. Kocen, A. M. LaPointe, M. Delferro, G. W. Coates, *J. Am. Chem. Soc.* **2022**, *144*, 23280–23285.
[29] N. Morlanés, S. G. Kavitake, D. C. Rosenfeld, J.-M. Basset, *ACS Catal.* **2019**, *9*, 1274–1282.
[30] K. Faust, P. Denifl, M. Hapke, *ChemCatChem* **2023**, *15*, e202300310.
[31] L. D. Ellis, N. A. Rorrer, K. P. Sullivan, M. Otto, J. E. McGeehan, Y. Román-Leshkov, N. Wierckx, G. T. Beckham, *Nature Catalysis* **2021**, *4*, 539–556.
[32] W. Zhang, S. Kim, L. Wahl, R. Khare, L. Hale, J. Hu, D. M. Camaioni, O. Y. Gutiérrez, Y. Liu, J. A. Lercher, *Science* **2023**, *379*, 807–811.
[33] P. Erdmann, L. Greb, *Angew. Chem. Int. Ed.* **2022**, *61*, e202114550.
[34] J. M. Hogg, L. C. Brown, K. Matuszek, P. Latos, A. Chrobok, M. Swadźba-Kwaśny, *Dalton Trans.* **2017**, *46*, 11561–11574.
[35] J. R. Gaffen, J. N. Bentley, L. C. Torres, C. Chu, T. Baumgartner, C. B. Caputo, *Chem* **2019**, *5*, 1567–1583.
[36] A. R. Jupp, T. C. Johnstone, D. W. Stephan, *Dalton Trans.* **2018**, *47*, 7029–7035.
[37] S. Borghèse, M. Haouas, J. Sommer, F. Taulelle, *J. Catal.* **2013**, *305*, 130–134.
[38] I. Mastalski, N. Sidhu, A. Zolghadr, S. Maduskar, B. Patel, S. Uppili, T. Go, Z. Wang, M. Neurock, P. J. Dauenhauer, *Chem. Mater.* **2023**, *35*, 3628–3639.
[39] R. W. J. Westerhout, J. Waanders, J. A. M. Kuipers, W. P. M. van Swaaij, *Ind. Eng. Chem. Res.* **1997**, *36*, 1955–1964.
[40] I. Akhrem, A. Orlinkov, *Chem. Rev.* **2007**, *107*, 2037–2079.
[41] R. Gallo, V. Lazzeri, *Appl. Catal. A* **1996**, *146*, 87–106.
[42] G. A. Olah, O. Farooq, Q. Wang, A. H. Wu, *J. Org. Chem.* **1990**, *55*, 1224–1227.
[43] S. Aschauer, L. Schilder, W. Korth, S. Fritschi, A. Jess, *Catal. Lett.* **2011**, *141*, 1405.
[44] L. Wu, R. Zhang, Y. Zhang, H. Liu, Z. Liu, C. Xu, X. Meng, *Ind. Eng. Chem. Res.* **2021**, *60*, 1155–1163.
[45] H. Nöth, R. Rurländer, P. Wolfgardt, *Z. Naturforsch. B.* **1982**, *37*, 29–37.
[46] J. P. Perdew, K. Burke, M. Ernzerhof, *Phys. Rev. Lett.* **1996**, *77*, 3865–3868.
[47] S. Grimme, W. Hujo, B. Kirchner, *Phys. Chem. Chem. Phys.* **2012**, *14*, 4875–4883.
[48] T. D. Kühne, M. Iannuzzi, M. Del Ben, V. V. Rybkin, P. Seewald, F. Stein, T. Laino, R. Z. Khaliullin, O. Schütt, F. Schiffmann, D. Golze, J. Wilhelm, S. Chulkov, M. H. Bani-Hashemian, V. Weber, U. Borštnik, M. Taillefumier, A. S.

Jakobovits, A. Lazzaro, H. Pabst, T. Müller, R. Schade, M. Guidon, S. Andermatt, N. Holmberg, G. K. Schenter, A. Hehn, A. Bussy, F. Belleflamme, G. Tabacchi, A. Glöß, M. Lass, I. Bethune, C. J. Mundy, C. Plessl, M. Watkins, J. VandeVondele, M. Krack, J. Hutter, *J. Chem. Phys.* **2020**, *152*, 194103.

[49] S. Goedecker, M. Teter, J. Hutter, *Phys. Rev. B* **1996**, *54*, 1703–1710.

[50] E. A. Carter, G. Ciccotti, J. T. Hynes, R. Kapral, *Chem. Phys. Lett.* **1989**, *156*, 472–477.

Manuscript received: December 18, 2023
Accepted manuscript online: March 3, 2024
Version of record online: March 15, 2024